Available online at www.sciencedirect.com
SCIENCE DIRECT®
Journal of Solid State Chemistry 178 (2005) 3256–3264
JOURNAL OF SOLID STATE CHEMISTRY
www.elsevier.com/locate/jssc

In situ neutron powder diffraction investigation of the hydration of tricalcium aluminate in the presence of gypsum

M.R. Hartman*, R. Berliner

University of Michigan, Ann Arbor, MI 48109, USA

Received 4 May 2005; received in revised form 26 July 2005; accepted 31 July 2005
Available online 16 September 2005

Abstract

The hydration of a 1:3 molar ratio of tricalcium aluminate, $Ca_3Al_2O_6$, to gypsum, $CaSO_4 \cdot 2D_2O$, was investigated at temperatures of 25, 50, and 80 °C using time-of-flight powder neutron diffraction combined with multiphase Rietveld structural refinement. It was shown that ettringite, $Ca_6[Al(OD)_6]_2(SO_4)_3 \cdot \sim 26D_2O$, was the first and only hydration product of the system, in contrast to a prior investigation which suggested the occurrence of a precursor phase prior to the formation of ettringite. Kinetics data showed that the hydration reaction is very sensitive to temperature: hydration at 25 °C was characterized by a single kinetic regime while hydration at higher temperatures consisted of two distinct kinetic regimes. The presence of two kinetic regimes was attributed to a change in either the dimensionality of the growth process or a change in the rate controlling mechanism in the hydration reaction.

Keywords: Cement hydration; Neutron powder diffraction; Hydration products; Calcium aluminate cement; Gypsum; Ettringite

1. Introduction

Cement-based materials pervade the modern infrastructure, yet despite their prevalence, many fundamental questions regarding the complex chemical reactions that occur during the formation and curing of these products remain. The initial hydration process is particularly complicated as a result of multiple, simultaneous, chemical reactions. One of the initial hydration reactions is that of the tricalcium aluminate phase, $Ca_3Al_2O_6$, of ordinary Portland cements. Although typical cements contain only ~10 wt% of the tricalcium aluminate phase, this phase is extremely reactive in the presence of water, and it is necessary to slow its hydration to allow for a workable cement and avoid the condition known as flash-set. To slow the hydration reaction of the tricalcium aluminate phase, retarding agents are added to the cement powder prior to hydration. A popular retarder is gypsum, $CaSO_4 \cdot 2H_2O$, which, when added in sufficient quantities slows the hydration. The actual retarding mechanism remains a question of some debate, but the formation of ettringite during the hydration of tricalcium aluminate in the presence gypsum is well established.

Christensen et al. [1] performed a neutron scattering investigation of the hydration of tricalcium aluminate in the presence of gypsum and hemihydrate. The formation of ettringite was observed but was found to be preceded by an unknown precursor phase. This precursor phase could be indexed to the ettringite unit cell, but the reflection intensities were different than those expected for ettringite. Performance of the experiment under similar conditions, using X-ray diffraction, did not reveal the precursor phase, suggesting that the precursor was a modification of the orientation of the water or hydroxyl molecules within ettringite, which contribute strongly to the neutron diffraction signal but only weakly to that due to X-rays. A tricalcium aluminate-to-gypsum molar ratio of 1:3 was investigated at 60 °C, and

*Corresponding author. National Institute of Standards and Technology, 100 Bureau Drive, MS 8562, Gaithersburg, MD 20899, USA. Fax: +1 301 921 9847.
E-mail address: michael.hartman@nist.gov (M.R. Hartman).

0022-4596/$ - see front matter © 2005 Elsevier Inc. All rights reserved.
doi:10.1016/j.jssc.2005.07.034

a tricalcium aluminate-to-gypsum molar ratio of 10:1.72 was investigated for temperatures ranging from 27 to 93 °C. For the hydration at 60 °C, only the precursor phase was observed during the 6 h observation period. In the investigation at 27 °C, the precursor was noted to exist for a period of ~8 h, at which time it was converted to ettringite over the course of the subsequent 2 h.

The present study reinvestigates the experiments of Christensen et al., using time-of-flight (TOF) neutron diffraction, with the aim of identifying the precursor and determining its structure, using multiphase Rietveld structure refinement methods [2]. A 1:3 tricalcium aluminate-to-gypsum molar ratio was investigated at 25, 50, and 80 °C. Ettringite was the only crystalline hydration product present, and the precursor phase noted by Christensen et al. was not observed.

2. Experimental procedure

2.1. Preparation and characterization of reactants

The cubic tricalcium aluminate employed in this study was obtained from Construction Technology Laboratories Inc. [3]. Gypsum was purchased from Alfa Aesar [4] and deuterated by dehydration at 135 °C, followed by rehydration with D_2O. The dehydration/rehydration process was repeated three times with the final gypsum product allowed to dry over a saturated solution of LiCl in D_2O (11% RH). The gypsum was ground to a fine powder and the tricalcium aluminate was used in an as-received condition. Powder X-ray diffraction was used to characterize both the tricalcium aluminate and the gypsum prior to the hydration studies. Both materials compared well with reference powder diffraction patterns and no crystalline impurities were visible in the spectra.

2.2. Tricalcium aluminate hydration

Hydration studies were conducted on the Special Environment Powder Diffractometer (SEPD) [5] of the Intense Pulsed Neutron Source (IPNS) at the Argonne National Laboratory and on the High Intensity Powder Diffractometer (HIPD) at the Lujan Center of the Los Alamos Neutron Science Center (LANSCE) at the Los Alamos National Laboratory. The studies were performed in a specially designed mixing assembly, shown in Fig. 1, which allowed the samples to be mixed directly in the neutron beam under a controlled temperature and atmosphere.

Prior to the performance of the hydration studies, separate powder diffraction patterns of the tricalcium aluminate and the deuterated gypsum were obtained on both the SEPD and HIPD diffractometers. These patterns allowed not only for the characterization of the reactants but also provided the necessary crystallographic models for the subsequent analysis of the hydration data.

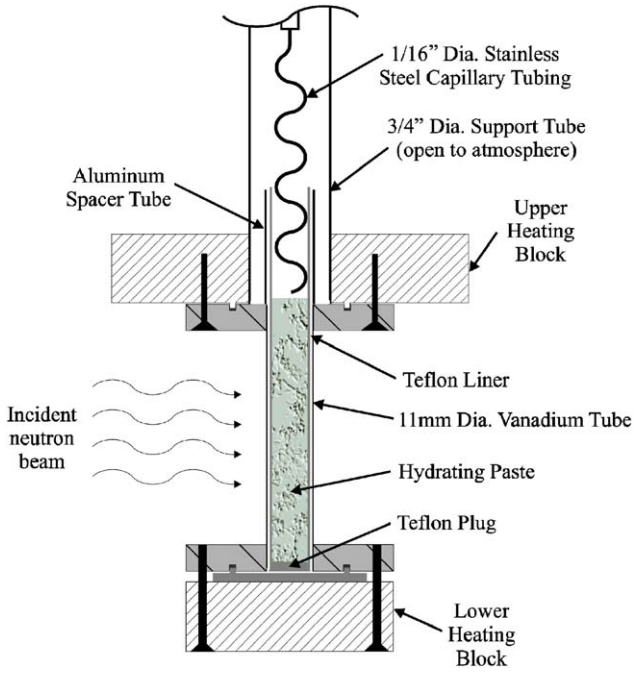

Fig. 1. Schematic illustration of the mixing assembly. The tubing connections and temperature diodes for the upper and lower heating blocks are not explicitly shown.

The hydration experiments were performed by first dry blending 6.662 mmol of tricalcium aluminate with 20.00 mmol of gypsum, a 1:3 molar ratio. After thorough mixing of the two powders they were loaded into the Teflon liner in the mixing section, located between the upper and lower heating blocks. The Teflon liner was used to prevent reaction of the hydrating paste with either the vanadium or aluminum used to construct the mixing assembly. Once loaded, the mixing section was bolted to the upper and lower heating blocks and the entire mixing assembly was loaded into the diffractometer, either SEPD or HIPD. A circulating constant-temperature water bath, connected to tubing on the upper and lower heating blocks, was set to the desired hydration temperature. The constant-temperature bath and the mixing assembly were allowed to equilibrate before proceeding further. D_2O was equilibrated at the hydration temperature by suspending a tightly sealed bottle in the reservoir of the constant-temperature bath. The hydration was conducted by injecting 7.50 ml of D_2O into the powder using a syringe connected to the 1/16″ capillary tube. The capillary tube, which was bent in a series of S-shaped bends at the end, was then lowered into the powder/water mixture and rotated by hand to create a homogeneous paste. The water-to-solids ratio of 1.55:1, used in this experiment, is higher than that for a typical cement hydration. It was chosen

to permit a workable paste with a sufficient amount of water to allow the reaction to go to completion while compensating for evaporative losses throughout the experiment. The water-to-solids ratio in the study by Christensen et al. [1] was 1.40:1 (1.27:1 using the density of water in lieu of D_2O). Once the paste had been evenly mixed, typically 1 min of constant rotation, the capillary tube was retracted and mechanically held above the paste to prevent any undesired diffraction signals. Data acquisition was initiated with a typical time delay of 5 min from the injection of D_2O to the start of data collection. To minimize the interaction of CO_2 with the hydrating paste, a nitrogen gas flow of 25 cm^3/min was maintained through the capillary tube throughout the hydration sequence with the exhaust gas vented to atmosphere. The hydration temperature was held constant, ± 1 °C, by the circulating constant-temperature bath.

Hydration studies were conducted at temperatures of 25, 50, and 80 °C. The studies at 25 and 50 °C were performed on the SEPD instrument at IPNS while the study at 80 °C was conducted on the HIPD instrument at LANSCE. Data for the 25 and 50 °C hydrations were collected in 30-min data sets with a total duration of 18 and 23 h, respectively. The 80 °C hydration data were collected in 20-min data sets for a total duration of 15 h.

3. Results and discussion

3.1. Analysis of hydration studies

Data from the hydration studies were subjected to a multiphase Rietveld crystal structure refinement, denoted simply as structural refinement from this point forward, using the GSAS computer code [6] as implemented in EXPGUI [7]. The structural refinement applies a non-linear least-squares fitting of a set of crystalline structural models to the diffraction data. The structural models are modified and compared to the data in an iterative fashion until close agreement between the models and the data is achieved. The crystallographic model for gypsum was based on the neutron powder diffraction study of Pedersen and Semmingsen [8], while that for tricalcium aluminate was taken from the study by Mondal and Jeffrey [9]. The recent TOF neutron powder diffraction work by Hartman and Berliner [10] provided the crystalline model for ettringite. In each phase, the cell parameters, isotropic thermal parameters, atomic positions, and peak profile parameters were refined. In addition, the deuterium occupation in the gypsum phase was refined to account for imperfect deuteration of the material.

To improve the statistical quality of the data, data from the hydrations at 25 and 50 °C were grouped into 2-h data sets by combining four individual 30-min data sets. In a similar manner, the data for the hydration at 80 °C were grouped into 80-min data sets by combining four separate 20-min data sets. Data from the $\pm 44°$, $\pm 90°$, and $\pm 145°$ SEPD detector banks were simultaneously used in refining the data obtained at 25 and 50 °C, while data from the $\pm 40°$, $\pm 90°$, and $\pm 153°$ HIPD detector banks were simultaneously used in refining the hydration at 80 °C. The fit of the multiphase structural refinement to the last data set for each hydration sequence is shown in Figs. 2–4 for the hydrations at 25, 50, and 80 °C, respectively. The difference in appearance of the powder diffraction data in Fig. 4, as compared to that in Figs. 2 and 3, is a result of differences in the diffractometers used to monitor the hydration and not a difference in the hydration itself. The multiphase structural refinements of the other hydration data sets were of similar quality, as demonstrated in Table 1. Figs. 5–7 illustrate the time evolution of the diffraction data, with the modeled background subtracted, for a region of reflections ranging from 0.24 to 0.31 nm, for the hydrations at 25, 50, and 80 °C, respectively. This particular region was chosen because it contains intense reflections from all three phases, allowing ready visualization of changes in intensity for the various crystalline phases present in the hydration reaction. For the hydration at 25 °C, shown in Fig. 5, the tricalcium aluminate and gypsum peaks remain essentially constant while the ettringite (216) peak, a very intense ettringite reflection, is just starting to become visible to the eye in the diffraction patterns at the end of the sequence. In the hydration at 50 °C, depicted in Fig. 6, the presence of ettringite is much more apparent, with several reflections clearly visible in the final diffraction pattern. At 50 °C, there are also noticeable changes in the tricalcium aluminate and gypsum peaks, signifying their consumption as the hydration reaction proceeds. The growth of ettringite and depletion of both tricalcium aluminate and gypsum is most apparent for the hydration at 80 °C, shown in Fig. 7. Here, in the final pattern, the ettringite reflections have intensities which exceed those of either tricalcium aluminate or gypsum, and the tricalcium aluminate and gypsum reflection intensities are much reduced relative to the initial diffraction pattern.

The changes in reflection intensities of the crystalline phases for the hydration at 50 °C are shown in Fig. 8. The phase intensities extracted from the multiphase structural refinement have been normalized by the relationship,

$$I'_n(t_i) = \left(\frac{1}{\text{Monitor}}\right) * \left(\frac{I_n(t_i) * Z_n}{I_{\text{Tricalcium Aluminate}}(t_0) * Z_{\text{Tricalcium Aluminate}}}\right), \quad (1)$$

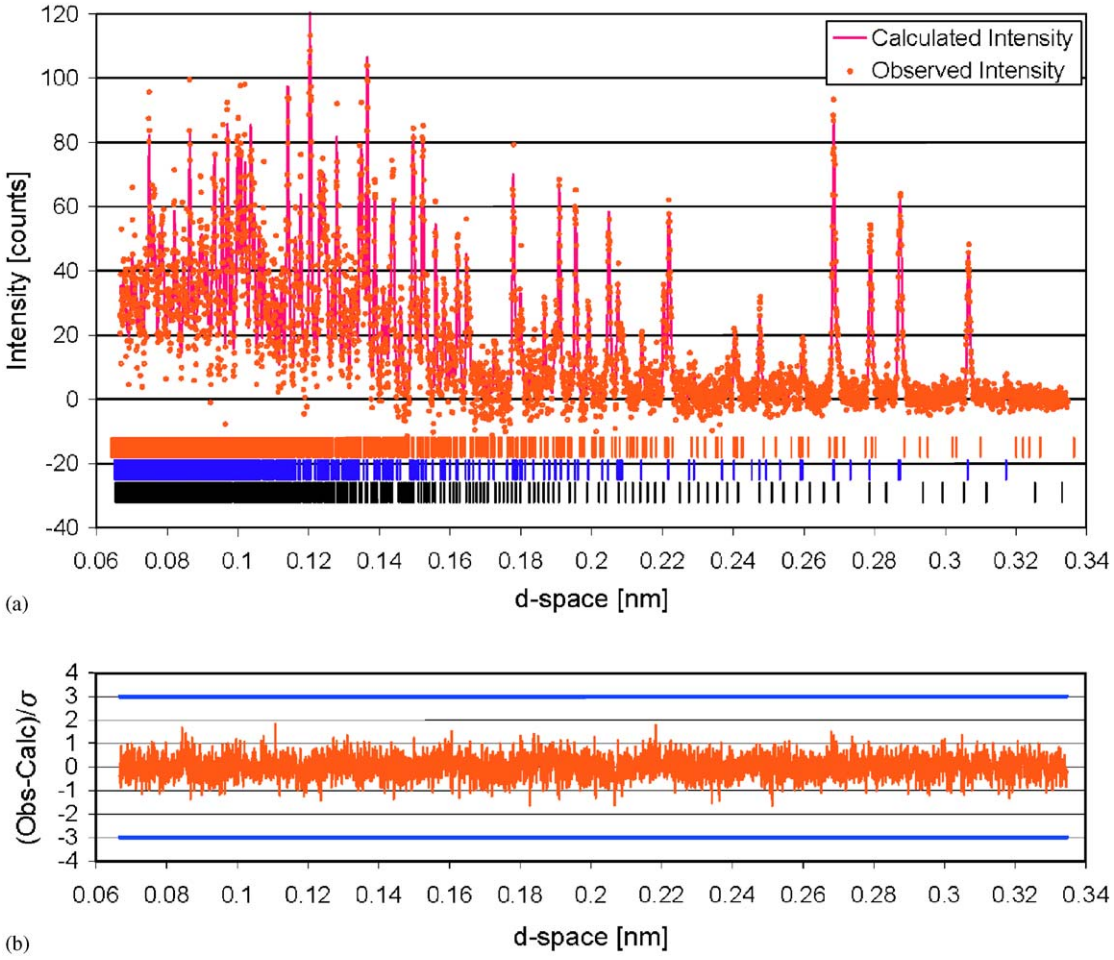

Fig. 2. (a) Fit of the multiphase structural refinement to the +145° SEPD detector data for data set 9 of the hydration at 25 °C with the modeled background subtracted. The median time of the data set is 17.03 h from the initiation of the hydration. Reflection locations for ettringite (blue), gypsum (red), and tricalcium aluminate (black) are represented by vertical lines positioned below the fitted data. (b) The error in the multiphase fit weighted by the uncertainty in the observed intensity. Solid orange lines are shown at $\pm 3\sigma$.

where I_n is the scale factor for the nth phase of the multiphase structural refinement, t_i is the time corresponding to the ith data set, Z_n equals the number of formula units per unit cell of phase n, and Monitor accounts for changes in the incident neutron beam intensity from data set to data set. The product $I_n * Z_n$ is the number of moles of the nth phase present. For a given phase, a normalized intensity is obtained for each detector bank used in the refinement, and Fig. 8 displays the arithmetic average of the normalized intensities as a function of time, for all detector banks used in the analysis. The tricalcium aluminate phase intensity at t_o for each detector bank was approximated by using the phase intensity for tricalcium aluminate from the first multiphase structural refinement. As a result of this normalization process, the plotted intensities approximate the number of moles of a given phase per initial mole of tricalcium aluminate. This correspondence is only approximate as a result of the consumption of some amount of the tricalcium aluminate within the first data set of the hydration. In Fig. 8, the intensities of tricalcium aluminate and gypsum are observed to monotonically decrease while that of the ettringite phase increases steadily.

Inspection of the multiphase structural refinements for all three hydration sequences reveals that the hydration product of tricalcium aluminate in the presence of gypsum is ettringite. In contrast to Christensen et al. [1], no indications of an unknown precursor phase are observed. Indeed, the structure factors for the ettringite produced in the hydration sequences agree well with those from the recent structural work by Hartman and Berliner [10] on synthetic phase-pure ettringite.

3.2. Kinetics of ettringite formation

Studies of the kinetics of ettringite formation by the reaction of tricalcium aluminate in the presence of gypsum have largely relied upon thermal calorimetry

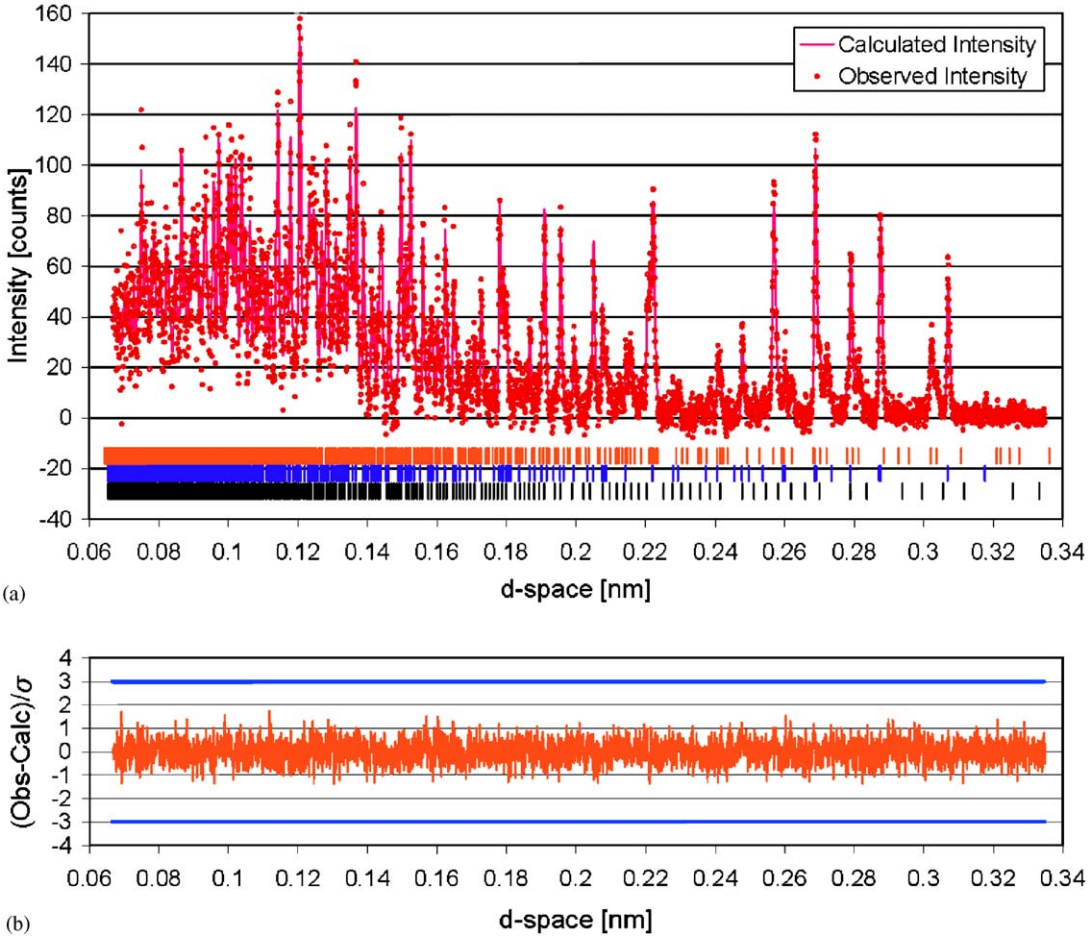

Fig. 3. (a) Fit of the multiphase structural refinement to the +145° SEPD detector data for data set 11 of the hydration at 50 °C with the modeled background subtracted. The median time of the data set is 21.63 h from the initiation of the hydration. Reflection locations for ettringite (blue), gypsum (red), and tricalcium aluminate (black) are represented by vertical lines positioned below the fitted data. (b) The error in the multiphase fit weighted by the uncertainty in the observed intensity. Solid orange lines are shown at $\pm 3\sigma$.

[11,12] and X-ray diffraction [13,14]. Thermal calorimetry is a non-invasive technique, but its analysis is complicated by the occurrence of other reactions occurring concurrently with the formation of ettringite. Accurate estimates of the kinetics of ettringite formation are then reliant upon properly accounting for all other simultaneous exothermic and endothermic chemical processes. X-ray diffraction studies have been utilized to determine time-resolved information on the kinetics of ettringite formation, but this method requires that the hydration reaction be stopped, typically by washing the hydrating paste in alcohol, drying, and grinding the material to a fine powder for analysis. Neutron diffraction analysis offers the possibility of observing, in situ, the growth of ettringite throughout the hydration process in an non-invasive manner. Some neutron diffraction investigations [1,15] have revealed the occurrence of ettringite in hydrating cement pastes, but they did not include a quantification of the reaction kinetics.

Although not the original intent of this study, information on the kinetics of ettringite formation during the hydration of tricalcium aluminate in the presence of gypsum may be extracted from the present data. Tables 2–4 give the phase intensity for ettringite, normalized using Eq. (1), for the hydrations at 25, 50, and 80 °C, respectively. The initial 80-min data set for the hydration at 80 °C has been split into two 40-min data sets to allow for extraction of kinetics at earlier times in that particular hydration sequence.

For determination of the kinetic parameters, a generalized nucleation and growth model

$$-\ln(1-(\alpha-\alpha_o)) = k(t-t_o)^N, \quad (2)$$

used previously by Brown and LaCroix [14], was employed where α is the fractional degree of reaction, k is a reaction rate constant, t represents the hydration time, α_o and t_o correspond to the fractional degree of reaction and time, respectively, at which the current rate limiting process began, and the exponent N describes

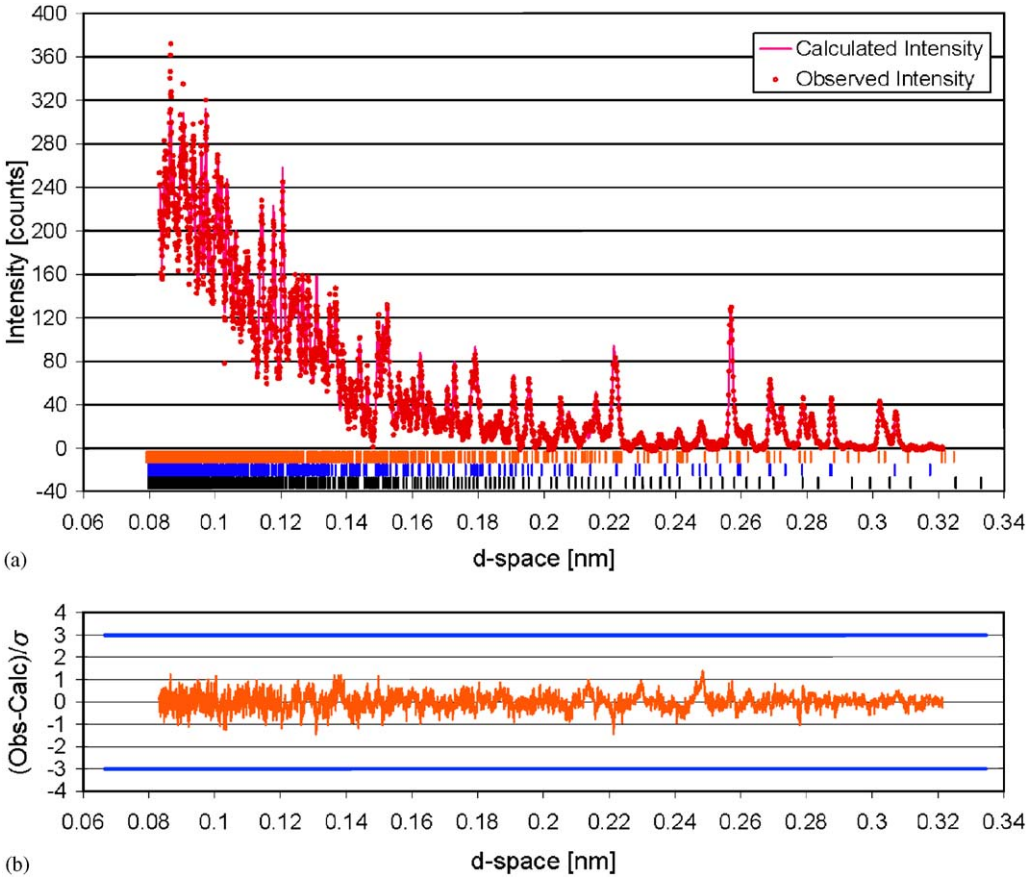

Fig. 4. (a) Fit of the multiphase structural refinement to the +153° HIPD detector data for data set 6 of the hydration at 80 °C with the modeled background subtracted. The median time of the data set is 13.15 h from the initiation of the hydration. Reflection locations for ettringite (blue), gypsum (red), and tricalcium aluminate (black) are represented by vertical lines positioned below the fitted data. (b) The error in the multiphase fit weighted by the uncertainty in the observed intensity. Solid orange lines are shown at $\pm 3\sigma$.

the character of reaction. The exponent N may be further expanded as

$$N = (Q + P/S), \tag{3}$$

where Q represents the nucleation rate constant, P characterizes the dimensionality of the growth process, and S describes the rate controlling growth mechanism. The value of Q may range from 0 for zero nucleation rate to a value of 1 corresponding to a constant nucleation rate, with all intermediate values possible. P may assume values of 1, 2, or 3, depending upon the dimensionality of growth for the product. S takes on a value of 1 for a surface-controlled growth mechanism and a value of 2 for a diffusion-controlled growth mechanism.

A value of 1.0 was assumed for the infinite-time ettringite phase intensity, corresponding to the complete reaction of all of the initial tricalcium aluminate with gypsum and D_2O to form ettringite. Applying this assumption, the fractional degree of reaction, α, simply becomes the ettringite phase intensity from Eq. (1) for each hydration data set. Plots of $\ln(-\ln(1-\alpha))$ versus $\ln(t)$ for the hydrations at 25, 50, and 80 °C are shown in Fig. 9.

The hydration at 25 °C is characterized by a single kinetic regime and, assuming $\alpha_o = 0$ and $t_o = 0$, a fit of a straight line to the plotted data yields, $k = 3.38 \times 10^{-3}\,h^{-0.57}$ and $N = 0.57$. The exponent $N = 0.57$ is very similar to the value of 0.53 reported by Brown and LaCroix [14], who observed the hydration of a 1:3 molar ratio of tricalcium aluminate to hemihydrate for a period of 240 h at 25 °C. A value of N near 0.5 is suggestive of one-dimensional diffusion limited growth ($Q = 0$, $P = 1$, and $S = 2$) which is consistent with the acicular crystalline habit of ettringite.

The hydrations at 50 and 80 °C are both characterized by two distinct kinetic regimes. In the case of the hydration at 80 °C, there is some question as to whether the first kinetic regime is properly described as a result of limited data at early hydration times. The existence of multiple kinetic regimes for the early stages of ettringite formation during the hydration of tricalcium aluminate in the presence of gypsum has been noted previously by Mori and Minegishi [16]. For the hydration at 50 °C, the

Table 1
Summary of the fit of the multiphase structural refinement to the hydration data at various temperatures

Data set	Median time [h]	R_{wp}	R_p	Durbin-Watson statistic, d
Hydration at 25 °C:				
1	1.03	0.0303	0.0212	1.889
2	3.06	0.0298	0.0210	1.900
3	5.08	0.0300	0.0210	1.885
4	7.12	0.0300	0.0210	1.882
5	9.16	0.0300	0.0209	1.879
6	11.20	0.0297	0.0207	1.934
7	13.23	0.0299	0.0209	1.860
8	15.27	0.0299	0.0210	1.894
9	17.03	0.0350	0.0244	1.928
Hydration at 50 °C:				
1	1.08	0.0301	0.0210	1.884
2	3.23	0.0305	0.0212	1.878
3	5.32	0.0305	0.0213	1.894
4	7.34	0.0308	0.0214	1.892
5	9.37	0.0302	0.0211	1.881
6	11.40	0.0303	0.0210	1.860
7	13.43	0.0307	0.0215	1.883
8	15.45	0.0307	0.0215	1.853
9	17.48	0.0306	0.0213	1.853
10	19.56	0.0308	0.0216	1.838
11	21.63	0.0307	0.0215	1.842
Hydration at 80 °C				
1	1.04	0.0134	0.0092	1.218
2	3.39	0.0130	0.0093	1.224
3	5.63	0.0131	0.0091	1.182
4	8.08	0.0144	0.0099	1.123
5	10.68	0.0148	0.0100	1.086
6	13.15	0.0140	0.0099	1.205

The statistical measures are defined as follows:

$$R_p \equiv \frac{\sum |I_{Observed} - I_{Calculated}|}{\sum I_{Observed}}$$

and

$$R_{wp} \equiv \left(\frac{\sum w(I_{Observed} - I_{Calculated})^2}{\sum w I_{Observed}^2} \right)^{1/2}.$$

The summations for R_p and R_{wp} extend over all data points.
Durbin-Watson statistic:

$$d = \frac{\sum_{i=2}^{N} (\Delta I_i - \Delta I_{i-1})^2}{\sum_{i=2}^{N} \Delta I_i^2},$$

where

$$\Delta I_i = I_{Observed} - I_{Calculated}$$

at the ith data point and the summations are over all N data points.

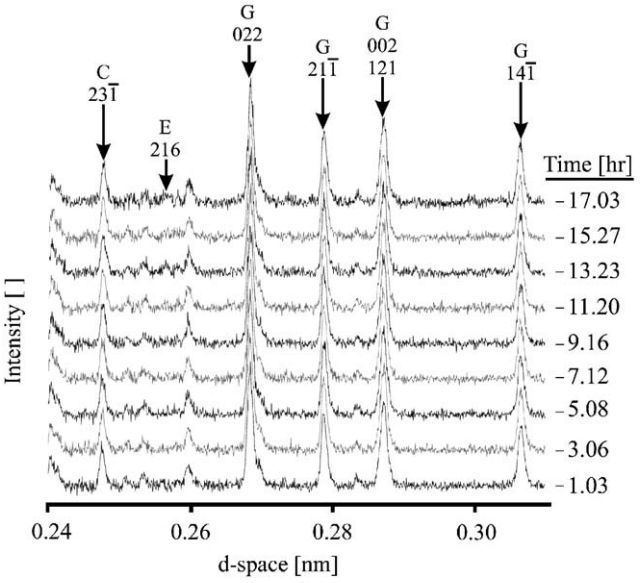

Fig. 5. Time evolution of the +145° SEPD detector diffraction data for the hydration at 25 °C. Prominent reflections are indicated for tricalcium aluminate (C), ettringite (E), and gypsum (G). The values of time, given to the right of each diffraction pattern, represent the median time since the start of hydration for the diffraction pattern.

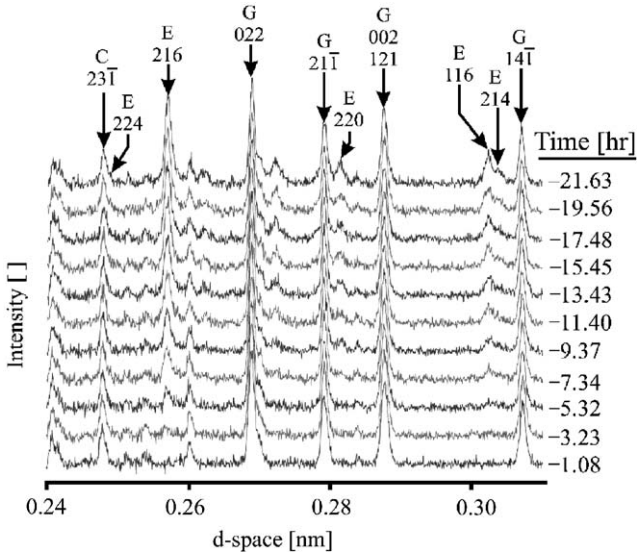

Fig. 6. Time evolution of +145° SEPD detector diffraction data for the hydration at 50 °C. Prominent reflections are indicated for tricalcium aluminate (C), ettringite (E), and gypsum (G). The values of time, given to the right of each diffraction pattern, represent the median time since the start of hydration for the diffraction pattern.

first kinetic regime was analyzed by assuming $\alpha_o = 0$ and $t_o = 0$. A straight line fit to the data gives $k = 2.85 \times 10^{-3}\,h^{-1.60}$ and $N = 1.60$. Using $\alpha_o = 0.0684$ and $t_o = 7.34$ as the transition point between regions, the second kinetic region is characterized by $k = 9.15 \times 10^{-3}\,h^{-0.90}$ and $N = 0.90$. For the hydration at 80 °C, the analysis of the first kinetic regime yields $k = 4.89 \times 10^{-2}\,h^{-3.27}$ and $N = 3.27$, with $\alpha_o = 0$ and $t_o = 0$. For values of $\alpha_o = 0.0951$ and $t_o = 1.25$, the second kinetic regime had values of $k = 4.03 \times 10^{-2}\,h^{-0.69}$ and $N = 0.69$. Determination of unambiguous values for Q, P, and S in the exponent N for the hydrations at 50 and 80 °C is not possible without corroborating evidence, but it is quite clear that the

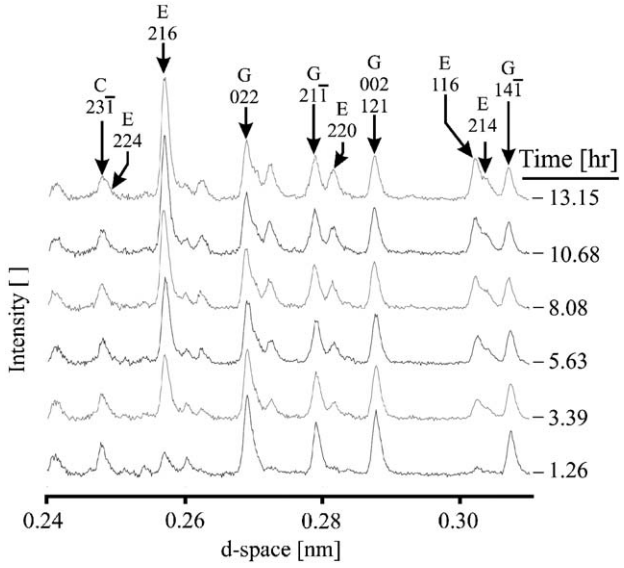

Fig. 7. Time evolution of +153° HIPD detector diffraction data for the hydration at 80 °C. Prominent reflections are indicated for tricalcium aluminate (C), ettringite (E), and gypsum (G). The values of time, given to the right of each diffraction pattern, represent the median time since the start of hydration for the diffraction pattern.

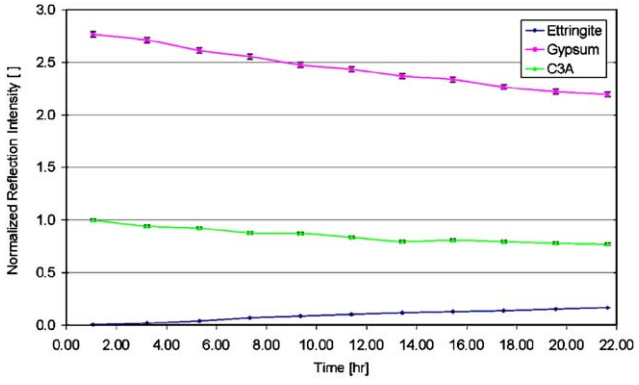

Fig. 8. Changes in the reflection intensities for the crystalline phases present in the hydration at 50 °C as a function of hydration time. The data points are plotted at the median time since the start of hydration for each set of data. Error bars at $\pm 1\sigma$ are included but are largely hidden beneath the data points.

character of the hydration reaction changes as a function of hydration time for the hydrations at elevated temperature.

4. Conclusion

The formation of ettringite during the hydration of a 1:3 molar ratio of tricalcium aluminate to gypsum has been investigated at temperatures of 25, 50, and 80 °C using powder neutron diffraction combined with a multiphase Rietveld crystal structure refinement. Analysis of the hydration data indicated that ettringite is the first and only hydration product of this system, and no indications of a precursor phase, noted in a previous study [1], were observed. Based upon a recent study, employing synchrotron X-ray powder diffraction, Christensen et al. [17] stated that the precursor noted in the

Table 2
Summary of ettringite phase intensity for the hydration at 25 °C

Data set	Median time [h]	Ettringite phase intensity [moles ettringite/initial mole of tricalcium aluminate]	Uncertainty in ettringite phase intensity, 1σ
1	1.03	0.0035	0.0003
2	3.06	0.0065	0.0003
3	5.08	0.0081	0.0004
4	7.12	0.0095	0.0003
5	9.16	0.0123	0.0004
6	11.20	0.0124	0.0003
7	13.23	0.0153	0.0004
8	15.27	0.0155	0.0004
9	17.03	0.0181	0.0006

Table 3
Summary of ettringite phase intensity for the hydration at 50 °C

Data set	Median time [h]	Ettringite phase intensity [moles ettringite/initial mole of tricalcium aluminate]	Uncertainty in ettringite phase intensity, 1σ
1	1.08	0.0032	0.0003
2	3.23	0.0180	0.0003
3	5.32	0.0392	0.0004
4	7.34	0.0684	0.0005
5	9.37	0.0850	0.0005
6	11.40	0.1014	0.0006
7	13.43	0.1164	0.0006
8	15.45	0.1267	0.0007
9	17.48	0.1363	0.0007
10	19.56	0.1512	0.0008
11	21.63	0.1652	0.0008

Table 4
Summary of ettringite phase intensity for the hydration at 80 °C

Data set	Median time [h]	Ettringite phase intensity [moles ettringite/initial mole of tricalcium aluminate]	Uncertainty in ettringite phase intensity, 1σ
1a	0.73	0.0179	0.0004
1b	1.25	0.0951	0.0005
2	3.39	0.1582	0.0003
3	5.63	0.2051	0.0004
4	8.08	0.2404	0.0004
5	10.68	0.2657	0.0005
6	13.15	0.2850	0.0005

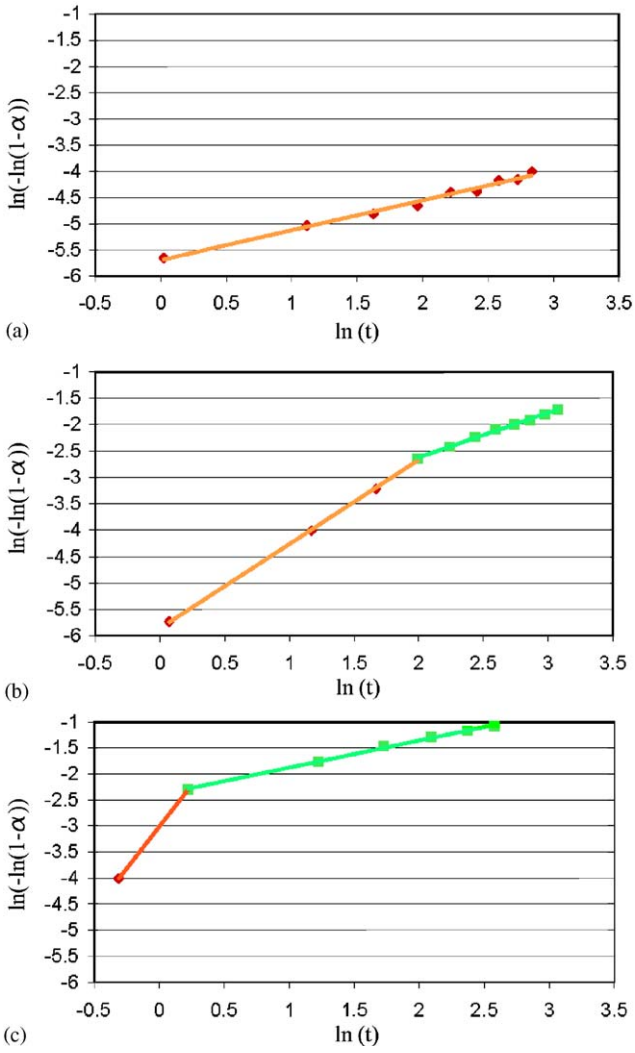

Fig. 9. Plot of $\ln(-\ln(1-\alpha))$ versus $\ln(t)$ for the hydration sequences at (a) 25 °C, (b) 50 °C, and (c) 80 °C.

earlier hydration study of the $C_{12}Al_{14}O_{33}$–$CaSO_4 \cdot 2D_2O$–D_2O system [1] was in fact ettringite which subsequently converted to monosulfate. However, they do not comment on the $C_3Al_2O_6$–$CaSO_4 \cdot 2D_2O$–D_2O system. The present investigation provides direct experimental evidence that ettringite is the hydration product of the latter system for the molar and water-to-solid ratios investigated and confirms that the precursor previously noted was indeed ettringite.

The kinetics of ettringite formation at 25 °C obeyed a single growth law during the period of observation, while the investigations at 50 and 80 °C were noted to contain two distinct kinetic regimes. Although the results of the kinetics analysis do not provide conclusive indication of the morphology or rate limiting mechanism for the formation of ettringite, they did indicate that the character of the reaction changes markedly during the initial stages of hydration within the temperature range investigated.

Acknowledgments

The authors wish to gratefully acknowledge the assistance of Dr. James Jorgensen, and Ms. Simine Short for their help in conducting the hydration experiments on the SEPD instrument and Dr. Anna Llobet-Megias for her assistance in conducting the hydration experiment on HIPD. Additionally, we thank Professor Michael Atzmon for many helpful discussions during the preparation of this manuscript. This work has benefited from the use of the Intense Pulsed Neutron Source at Argonne National Laboratory and the Los Alamos Science Center at the Los Alamos National Laboratory which are funded by the US Department of Energy under Contract W-31-109-ENG-38 and Contract W-7405-ENG-36, respectively. Funding for this work was provided in part by the National Science Foundation Grant CMS-0196400.

References

[1] A.N. Christensen, H. Fjellvåg, M.S. Lehmann, Acta Chem. Scand. A 40 (1986) 126–141.
[2] H.M. Rietveld, J. Appl. Cryst. 2 (1969) 65–71.
[3] Construction Technology Laboratories, Inc., 5420 Old Orchard Road, Skokie, IL 60077.
[4] Alfa Aesar, A Johnson Matthey Company, 30 Bond Street, Ward Hill, MA 01835-8099. Stock number 33301.
[5] J.D. Jorgensen, J. Faber, J.M. Carpenter, R.K. Crawford, J.R. Haumann, R.L. Hitterman, R. Kleb, G.E. Ostrowski, F.J. Rotella, T.G. Worlton, J. Appl. Cryst. 22 (1989) 321–333.
[6] A.C. Larson, R.B. Von Dreele, General Structure Analysis System (GSAS), Los Alamos National Laboratory Report LAUR 86-748, 2000.
[7] B.H. Toby, J. Appl. Cryst. 34 (2001) 210–213.
[8] B.F. Pedersen, D. Semmingsen, Acta Cryst. B 38 (1982) 1074–1077.
[9] P. Mondal, J.W. Jeffery, Acta Cryst. B 31 (1975) 689–697.
[10] M.R. Hartman, R. Berliner, Reinvestigation of the structure of ettringite by time-of-flight neutron powder diffraction techniques, Cement Concrete Res., in press.
[11] E. Gruszczscinski, P.W. Brown, J.V. Bothe Jr., Cement Concrete Res. 23 (1993) 981–987.
[12] B.A. Clark, P.W. Brown, Cement Concrete Res. 29 (1999) 1943–1948.
[13] P.K. Mehta, J. Am. Ceram. Soc. 56 (6) (1973) 315–319.
[14] P.W. Brown, P. LaCroix, Cement Concrete Res. 19 (1989) 879–884.
[15] M. Castellote, C. Alonso, C. Andrade, J. Campo, X. Turrillas, Appl. Phys. A 74 (2002) S1224–S1226.
[16] H. Mori, K. Minegishi, Effect of temperature on the early hydration of the system $3CaO \cdot Al_2O_3$–$CaSO_4 \cdot 2H_2O$–$Ca(OH)_2$–H_2O, Proceedings of the Fifth International Symposium on the Chemistry of Cement, Tokyo, 1968, pp. 349–361.
[17] A.N. Christensen, T.R. Jensen, J.C. Hanson, J. Solid State Chem. 177 (2004) 1944–1951.